International Journal of Modern Manufacturing Technologies
ISSN 2067–3604, Vol. XVI, No. 2 / 2024
https://doi.org/ 10.54684/ijmmt.2024.16.2.89

INVESTIGATING WEAR OF PIN FABRICATED BY PRESSURE-LESS SINTERING OF COPPER POWDER INTO 3D PRINTED CLAY MOULDS

Harshit K Dave[1], Savan D Fefar[2]

[1,2]Department of Mechanical Engineering, S. V. National Institute of Technology, Surat, Gujrat 395007, India

Corresponding author: Harshit K Dave, harshitkumar@yahoo.com

Abstract: Powder metallurgy (P/M) is a typical process for producing metal parts and metal matrix composites by employing powder-form materials. The main challenge to the economic viability of P/M components is the expense of die-making, especially when producing small quantities of parts. Pressure-less sintering is a promising approach in P/M, with the potential for efficient and cost-effective manufacturing through the use of customised dies produced through 3D printing. This study examines the wear characteristics of pressure-less sintered copper pins produced in 3D-printed clay moulds. The research focuses on Pin-On-Disk wear testing and microhardness to assess the component quality and to understand the wear rate of these pins under different loading conditions, viz. sliding velocities and applied load.
Moreover, the study aims to demonstrate the effectiveness of the combination of pressure-less sintering through 3D Printed clay moulds highlighting its potential for producing durable copper pins. Through a comprehensive investigation into the wear performance of components synthesized by the integration of pressure-less sintering and 3D printing technologies, known as Additive Manufacturing. Based on experimental investigation it has been observed that sliding speed and applied force have a direct impact on wear rate. In particular, the applied load has a major influence on the wear rate in pin-on-disc wear tests for the same sliding distance.

Key words: pressure-less sintering, copper, 3D printed clay moulds, additive manufacturing, wear rate

1. INTRODUCTION

Copper (Cu) and its alloys are commonly used in contacting machine parts. Due to its excellent mechanical, electrical and wear properties (Shakarappa et al., 2023) copper has found widespread use as a friction material in the aerospace, military, and marine transportation industries (Wang et al., 2023), (Safari et al., 2017). The development of advanced machinery toward higher weights and speeds requires copper-based friction materials to have improved properties, such as better resistance to wear. Moreover, wear, corrosion, and fatigue are common causes of mechanical component failure in machines, leading to malfunctions, lower efficiency, and component replacement (Maculotti et al., 2022).
Several sintering processes have been developed and widely employed, including spark plasma sintering (Torralba et al., 2014), microwave sintering (Xu et al., 2016) hot press sintering (Gao et al., 2020), cold-press sintering (Vakifahmetoglu, C. & Karacasulu, L., 2020), pressure-less sintering (Ott et al.,2021), etc. Numerous parameters associated with powder processing and powder morphologies can potentially influence the final part qualities obtained by powder-based manufacturing techniques. Typically, finer powder particles offer components higher density, improved microstructural characteristics, and superior mechanical properties compared to coarser particles. The proper selection of powder particle sizes results in reduced porosity and a significant improvement in both microstructural integrity and mechanical properties. The pressure-less sintering method can be used to sinter copper powder below the melting point; however, the resultant materials frequently contain voids, resulting in less than 90% theoretical density (Huang et al., 2023). Re-densification by re-pressing and re-sintering is a typical method for increasing density. The impact of load and sliding velocity on the friction and wear of Cu in dry conditions has been explored by many researchers. The analysis of Cu surface layers during dry friction indicates significant plastic deformation, leading to the formation of a fragmented structure in subsurface layers (Meshi et al., 2011). The pin-on-disc, or tribometer, is essential for wear and friction testing on additively produced materials, which determine their appropriateness for a variety of applications. Tribometers are used in wear and friction testing to study surface interactions under different situations. Safari et al. (2017) investigated the Pin-On-Disk (POD) wear behaviours of copper matrix composites enhanced with γ-Cu_5Zn_8 intermetallic nanoparticles. The samples were prepared by cold pressing at

800 MPa, then sintered via spark plasma sintering (SPS), and finally analysed for microstructural and mechanical properties. Vedrtnam et al. (2017) have also evaluated the wear characteristics of Al-SiC-Cu MMCs under various reinforcement levels, loads, sliding speeds, and distances by employing a POD setup. They observed that reinforcement levels have the highest impact, followed by applied load and sliding speed while sliding distance has minimal impact on wear characteristics. As highlighted in numerous scholarly works, the POD approach is consistently recommended as the most precise and, indeed, the preferred method for conducting wear tests across a diverse range of materials. Essential variations can be introduced during testing by including different process parameters. As a result, this method has emerged as one of the most valuable techniques in the field of wear testing (Kumar et al., 2021).
In the current research work, copper components have been created using pressure-less sintering of copper powder in 3D-printed clay moulds. These moulds are fabricated by using terracotta clay material which has firing temperature in the range of 1080°C-1180°C, making it suitable for withstanding higher sintering temperatures (Kurama et al., 2006), (Touolak & Nya, 2014). Components are produced by integrating the indirect AM route instead of the standard powder metallurgy sequence for compacting and sintering. This technique eliminates the step of the die-making process that is typically required for producing green parts using traditional methods.

2. MATERIALS AND METHODS

2.1. Sample fabrication

Initially, clay moulds are created using Material Extrusion (MEX) 3D printing technology, which uses a screw extrusion-based clay 3D printer (M/s Deltasys E-forming). There has been a growing interest in the use of clay for MEX in construction projects as well due to its environmentally friendly properties (Shubbar et al., 2019). Figure 1 (starting from a to g), depicts the process stages for obtaining a copper pin via pressure-less sintering of copper powder. The procedure uses an air cylinder system to compress clay past. To make the clay paste for moulding, 1kg of clay powder is manually combined with 300 ml of water. Once the required paste consistency has been attained, it is placed in a clay container.

Fig. 1. Process flow for sample fabrication

An oil-free compressor is used to deliver the pressure required to push the clay paste from the cylinder. To achieve the required material flow, the pressure is accurately regulated using a pressure-regulating valve. To start the sample fabrication procedure, a 3D model of the mould cavity, replicating the pin size, is created with Fusion 360 software's 2023 Education access version. This model is then converted to. stl format and loaded into the clay 3D printing program (Simplyfy3D) to generate the G-codes that are necessary for 3D printing. After printing, the moulds are air-dried for 24 hours and manually filled with electrolytic high-purity copper powder (≈99.9%, ≤ 50 μm). Sintering of copper powder-filled moulds is done in a coal-enhanced ceramic furnace with no external pressure to validate additive manufacturing principles. To maintain a reducing environment and avoid oxidation, the sintering temperature was maintained at 400°C for 20 minutes before reaching the ultimate sintering temperature of 850°C. Following the sintering process, the furnace is turned off, and the components are left inside to cool gradually, reducing the risk of thermal stress.

2.2. Design of Experiments

A series of pilot studies for the Pin-on-Disk wear test is conducted to identify the affecting process parameters. Two process parameters applied load (N) and sliding speed (In terms of rpm of the rotating disk) were considered with 3 levels while keeping the total sliding distance common for all test runs. Implemented a full factorial experimental design in conjunction with the Taguchi approach for signal-to-noise (S/N) ratio analysis to enhance the efficiency of conducting our wear measurement tests. This design incorporates two parameters, each characterized by three discrete levels, as described in Table 1.

Table 1. Wear Testing Process parameters with their levels

Levels/Parameter	Load (N)	Speed (rpm)	Constant Parameters
1	15	300	Sliding Distance = 1500 m
2	25	400	
3	35	500	

The evaluation of wear rate serves as the primary response to these experiments. Apart from this Micro hardness and microstructures of the specimens are recorded for detailed observation. Once the components are taken out of the furnace, the sintered parts are separated by carefully breaking the moulds by pressing on their side walls with a bench vice to allow the sintered copper piece to be separated. Figure 2 depicts the sintered copper pins after machining to obtain a uniform cylindrical pin shape for wear measurement testing. Moreover, this machining process also helps to remove the unevenness of surface area caused due to 3D printed layers impressions present on moulds.

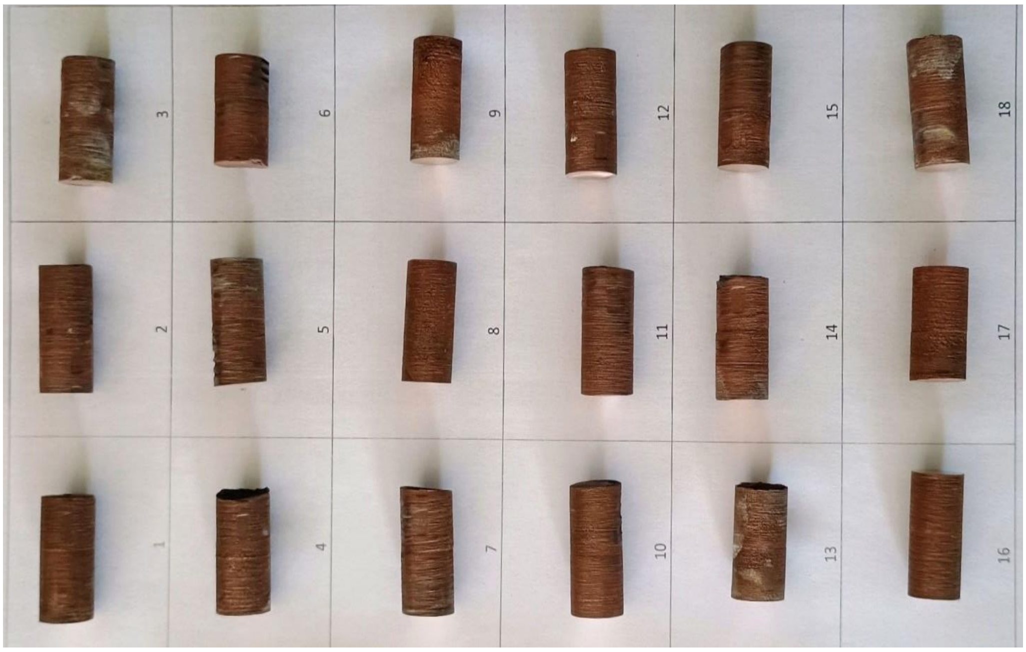

Fig. 2. Sintered copper pins after machining

After obtaining the cylindrical pin-shaped copper specimens, systematic testing and characterization procedures are executed. Before proceeding with the wear test, the sintered specimens are cleaned using a multistep polishing procedure. The specimen polishing process is first carefully performed with silicon carbide (SiC) sheets that have grit sizes ranging from 150 to 2000. This increasing range of grit sizes—150, 400, 600, 800, 1000, 1200, 1500, and 2000—allows for the surface roughness to be gradually refined, ultimately leading to the achievement of a flawlessly smooth surface. This rigorous polishing strategy is essential for setting up the specimens for subsequent characterization procedures because it removes surface flaws and inconsistencies, which maximizes the accuracy and reliability of the studies that follow.

2.3. Testing and Characterizations

The assessment of hardness and wear attributes of the specimens is facilitated through the utilization of the Vicker micro-Hardness test and the Pin-on-Disc Wear test respectively.

2.3.1. Micro hardness tests

The Vickers hardness test, also known as microhardness testing, uses an optical measurement system with low loads and a diamond indenter to measure and convert indentation into hardness values. It uses a diamond pyramid with a square base, where opposing sides converge at an angle of α = 136°, as the indenter. It is then pressed onto the specimen with a force of 50 g and held in place for 10 seconds, this standardised conduct ensures that surface hardness assessments are consistent and precise. The lengths of both diagonals of the resultant indentation are then measured optically. A Digital Vickers hardness tester (Model No. HWMMT-X7), as illustrated in Figure 3, enables the exact evaluation of surface hardness and a full assessment of material characteristics with precision.

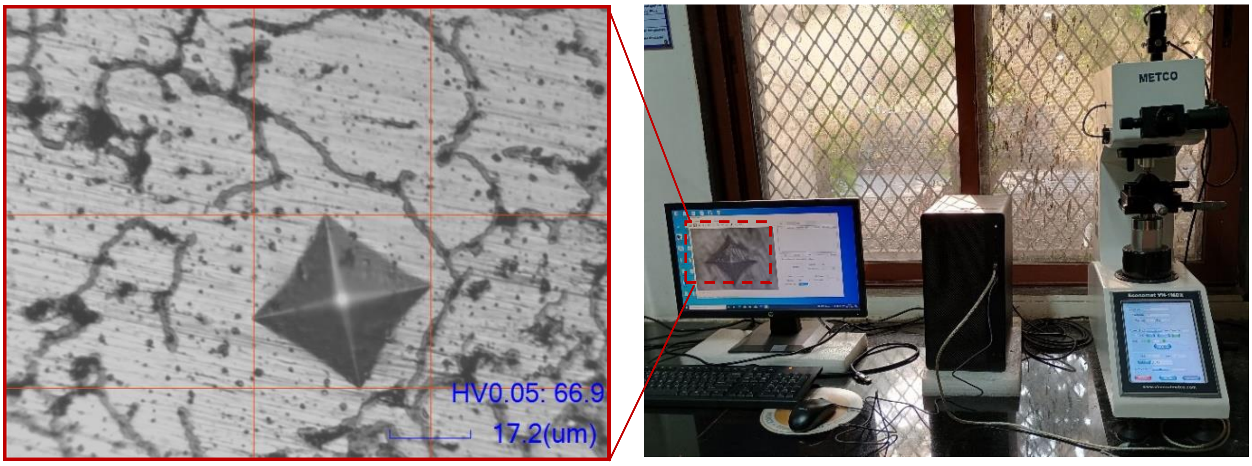

Fig. 3. Vicker hardness testing setup

To ensure comprehensive data collection, measurements are obtained from five distinct areas on each sample. Subsequently, the average of these measurements is calculated to mitigate any potential localized variations.

2.3.2. Wear Measurement

The TR-20LE Pin-on-Disc wear machine, manufactured by Ducom (India), was utilized for conducting dry wear tests following the ASTM G99 standard, as illustrated in Figure 4. In this experimental setup, the specimen, possessing a diameter of 10 mm, is affixed as a stationary pin for the wear test, while the steel disc rotates at a selected rpm. Under the specified load, the track diameter and total sliding distance remain constant, with values of 80 mm and 1500 m, respectively. The wear rate is calculated with the help of following Equation (1),

$$W = \frac{W_i - W_f}{P.d} \tag{1}$$

Where, W (g/N.m) represents wear rate, W_i (g) is sample mass before testing, W_f (g) indicates sample mass after testing, P (N) represents applied force, and d (m) represents track diameter.

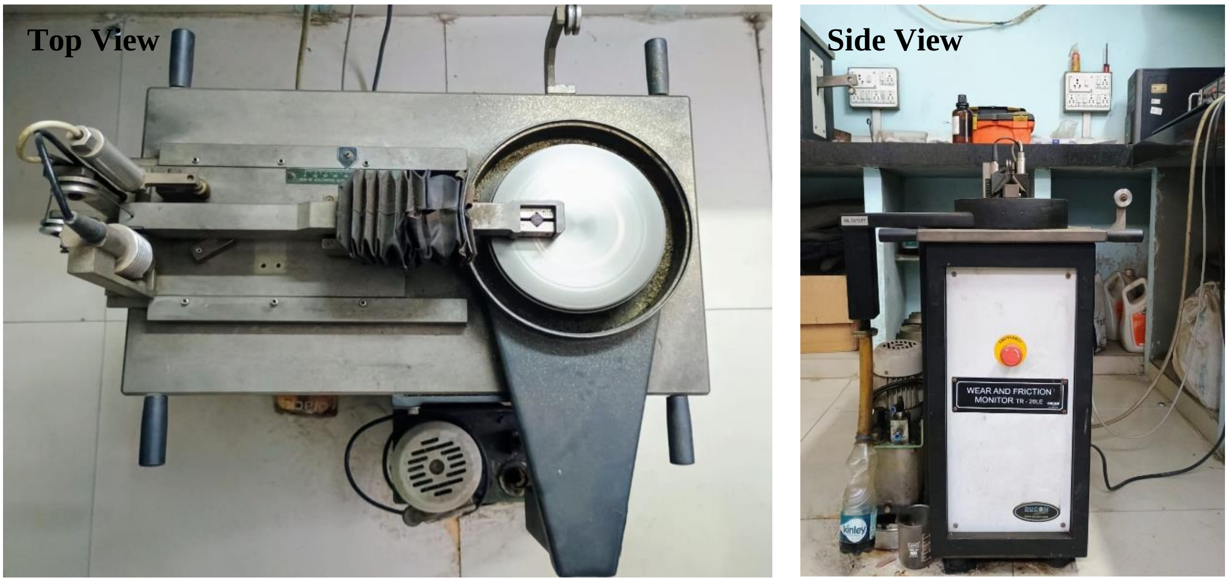

Fig. 4. Pin-On-Disk Wear Measurement Set-up.

Weight loss of each sample is recorded by using a digital analytical balance (M/S: Contech Instruments Ltd.) weight measurement instrument having the least count of 0.1 milligram.

3. RESULTS AND DISCUSSION

The outcomes of wear test experiments conducted on cylindrical sintered copper pin specimens is shown in Table 2, showing the measured output values for Wear Rate. Consistent with the principles of the full factorial design of experiments, a total of 9 experimental runs are considered, as detailed in Table 2. To enhance precision and reliability, two distinct sets of experiments are executed and the output of the wear rate is denoted as WR1 and WR2.

Table 2. Experimental results of Wear Testing

Sr.	Load (N)	Speed (rpm)	Micro-Hardness (HV)	Wear Rate (g/N.m)			
				W_{R1}	W_{R2}	W_R Mean	S/N Ratio (db)
1	15	300	48	0.0039	0.0038	0.0038	48.3285
2	15	400	46	0.0052	0.0056	0.0054	45.3924
3	15	500	47	0.0090	0.0085	0.0088	41.1598
4	25	300	52	0.0078	0.0081	0.0080	41.9927
5	25	400	47	0.0089	0.0093	0.0091	40.8192
6	25	500	48	0.0099	0.0104	0.0101	39.8921
7	35	300	52	0.0087	0.0086	0.0087	41.2310
8	35	400	48	0.0099	0.0097	0.0098	40.1565
9	35	500	49	0.0119	0.0114	0.0116	38.6921

As observed in Table 2, the highest microhardness obtained is 52 HV and the lowest wear rate obtained is 3.83 mg/N.m. Similar results for pure copper is also reported by (Ayyappadas et al., 2017), (Vignesh Babu & Kanagaraj, 2019), (Singh & Pandey, 2020). The difference between the initial and final weights of the composites after wear testing quantifies wear loss caused by the impact of solid particles. These experimental results are then transformed into signal-to-noise (S/N) ratios. For each combination of factor levels, the signal-to-noise (S/N) ratio is computed. The formula shown in equation (2) is employed for deriving the S/N ratio, adhering to the smaller-is-better criteria is as follows:

$$\eta = -10.\log\left[\sum \frac{y^2}{n}\right] \tag{2}$$

Where, Y represent the observed data, while n stands for the total number of observations. Figure 5, shows how process factors such as applied load and sliding speed affect wear, using the mean Signal to-Noise (S/N) Ratio. The main effect plot (as illustrated in Figure 5) is created by using the Minitab software with the help of experimental results data. Higher mean S/N ratio values help to identify the best parameter combination. As a result, the best wear combination is 15 N (applied load) and 300 rpm (slide speed) which results in minimum wear.

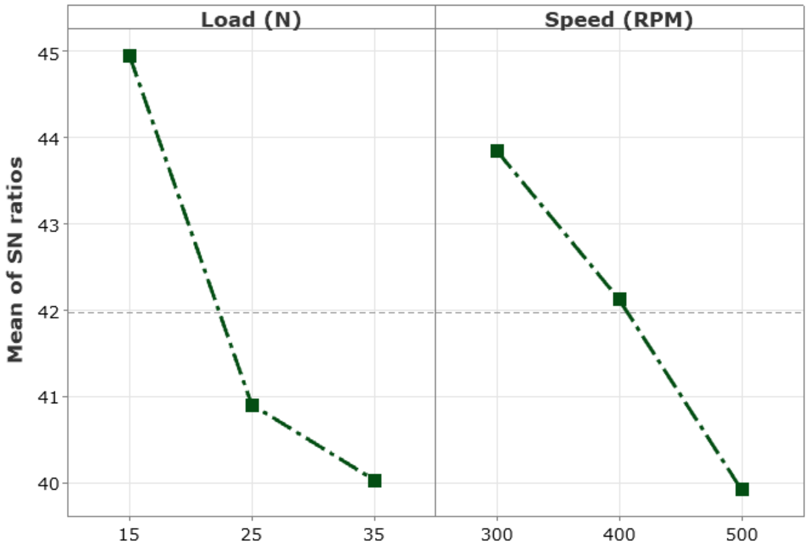

Fig. 5. Main effect plot of Load and Speed for mean S/N Ratio

The S/N curve for applied load exhibits the steepest incline rather than the speed process parameter, indicating its predominant impact on wear compared to speed. It is also evident from the ANOVA table (as described in Table 3) that the P value of the load factor is very low near 0.05 as compared to the speed factor. This also suggests the influence of load on wear rate is higher compared to speed.

Table 3. Analysis of Variance (ANOVA) for Wear Rate

Source	DF	Adj SS	Adj MS	F-Value	P-Value	Contribution
Load (N)	2	26.855	13.4275	23.06	0.006	58.01%
Speed (rpm)	2	17.110	8.5548	14.69	0.014	36.96%
Error	4	2.329	0.5822			5.03%
Total	8	46.294				100.00%

The wear rate is determined by both sliding speed and applied load, with sliding speed contributing approximately 37% and applied load contributing a considerable 58%, making it the predominant factor. However, sliding speed at higher rpm resulted in more wear compared to lower rpm. This could be the result of increased friction and heat at the contact area of the pin and disk during the test at the higher rpm. While the applied load effect is directly indicating the increased stress on the pin resulted in more worn-out copper pin specimens. Similar observation has been reported by (Zengin et al., 2019), (Tagimalek & Mahmoodi, 2023). The effect of wear process parameters on wear rate is illustrated in Figure 6 by analysing the data in Origin 2024 software. It shows the applied load on the X-axis, wear rate on the Y-axis, and sliding velocity rpm values in the form of lines containing wear rate results obtained at different speeds against each applied load setting value. With the increase of applied load and sliding speed, there is a significant increase in wear rate is observed. However, sliding speed is notably affecting less than the applied load.

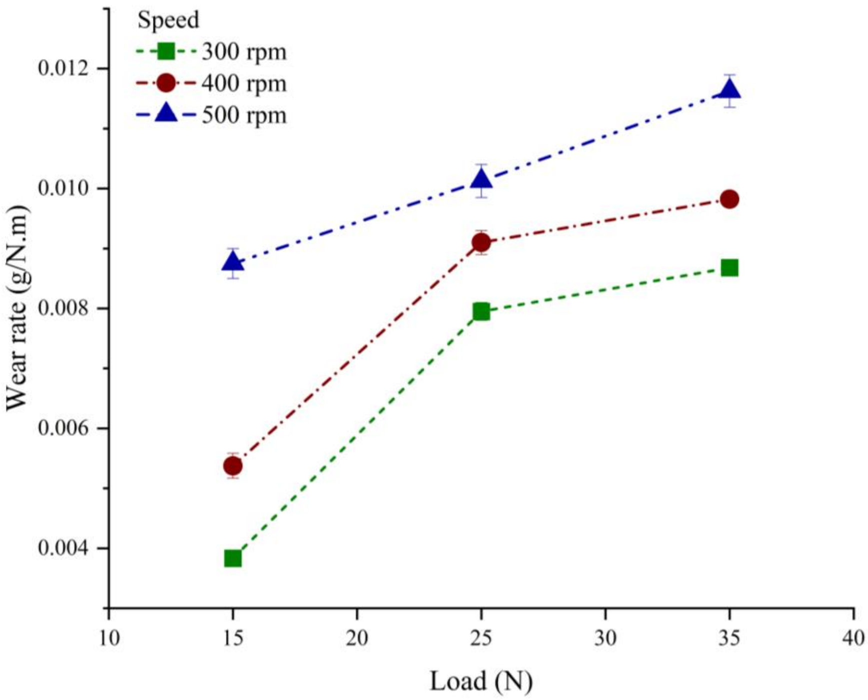

Fig. 6. Effect of wear process parameters on wear rate

Moreover, it is observed that the change in wear rate is very low when the applied load is 15 N. It can be assumed that when the applied load got increased the wear scare got enhanced rapidly resulting in higher wear rate with higher applied loading conditions along with higher sliding speed.

4. CONCLUSIONS

Copper specimens are efficiently produced by employing pressure-less sintering into 3D-printed clay moulds. For further examination of the quality of the resulting components, wear testing and microhardness measurement is evaluated.
In the current study, an analysis of the wear rate was conducted, involving variations in applied load and sliding speed within the Pin-On-Disk wear measurement technique.
Results of the experimental study, suggest the impact of applied load is more dominant as compared to sliding velocity for the wear rate.
Highest wear rate is observed when the applied load and sliding velocity are kept at higher levels, i.e., at 35 N and 500 rpm. Similarly, the lowest wear rate is observed when the applied load and sliding speed are at their lower levels, i.e. 15N and 300 rpm.
This wear rate behaviour suggests the higher degradation and worn-out of the contacting surface of the pin area when subjected to higher stress due to higher applied load and increased heat at the pin and disk contact at higher sliding velocity.

Funding: This paper has received no external funding
Conflicts of Interest: There is no conflict of interest.

REFERENCES

1. A.A Shubbar, M. Sadique, P. Kot, and W. Atherton (2019), *Future of clay-based construction materials – A review*, Constr Build Mater, 210, 172–187, doi: 10.1016/j.conbuildmat.2019.03.206.
2. Ayyappadas C., Muthuchamy A., Raja Annamalai A., Agrawal, D. K. (2017). *An investigation on the effect of sintering mode on various properties of copper-graphene metal matrix composite*, Advanced Powder Technology, 28(7), 1760–1768. https://doi.org/10.1016/j.apt.2017.04.013
3. Gao, J., Yang, L., Guo, S., Jia, L., Wang (2020). *Fabrication of Fe60Cu40 pre-alloy bonded composites for diamond tools by microwave hot press sintering*. Journal of Materials Research and Technology/Journal of Materials Research and Technology, 9(4), 8905–8915. doi.org/10.1016/j.jmrt.2020.06.001
4. Huang, W., Yu, H., Wang, L., Wu, X., Ouyang, C., Zhang, Y., He, J. (2023). *State of the art and prospects in sliver- and copper-matrix composite electrical contact materials*. Materials Today Communications, 37,

107256–107256. https://doi.org/10.1016/j.mtcomm.2023.107256
5. Kumar, A., Choudhary, A., Tiwari, A., James, C., Kumar, H., Kumar Arora, P., Akhtar Khan, S. (2021). *An investigation on wear characteristics of additive manufacturing materials*. Materials Today: Proceedings, 47, 3654–3660. https://doi.org/10.1016/j.matpr.2021.01.263
6. Kurama, S., Kara, A., & Kurama, H. (2006). *The effect of boron waste in phase and microstructural development of a terracotta body during firing*. Journal of the European Ceramic Society, 26(4–5), 755–760. https://doi.org/10.1016/j.jeurceramsoc.2005.07.039
7. Maculotti, G., Goti, E., Genta, G., Mazza, L., & Galetto, M. (2022). *Uncertainty-based comparison of conventional and surface topography-based methods for wear volume evaluation in pin-on-disc tribological test*. Tribology International, 165, 107260. https://doi.org/10.1016/j.triboint.2021.107260
8. Meshi, L., Shmuel Samuha, Cohen, S. R., Laikhtman, A., Moshkovich, A., Vladislav Perfilyev, Igor Lapsker, Rapoport, L. (2011). *Dislocation structure and hardness of surface layers under friction of copper in different lubricant conditions*. Acta Materialia, 59(1), 342–348. https://doi.org/10.1016/j.actamat.2010.09.038
9. Ott, J., Burghardt, A., Britz, D., & Mücklich, F. (2021). *Influence of porosity and impurities on the thermal conductivity of pressure-less sintered Cu powder green bodies*. Powder Metallurgy, 64(2), 85–96. https://doi.org/10.1080/00325899.2021.1871806
10. Safari, F., Azari Khosroshahi, R., & Zolriasatein (2017). *Wear behavior of copper matrix composites reinforced by γ-Cu5Zn8 nanoparticles*. Powder Technology, 318, 549–557. doi.org/10.1016/j.powtec.2017.06.032
11. Shakarappa, R., Arul Peter, A., Rathna Kumar, P., Mallikarjuna, M. V., & Padmanabhan, S. (2023). Microstructure mechanical behavior of Cu-Sn alloy reinforced with Al2o3 and Graphene metal matrix composite. Materials Today: Proceedings, 92, 1122–1128. https://doi.org/10.1016/j.matpr.2023.05.145
12. Singh, G., & Pandey, P. M. (2020). Rapid manufacturing of copper-graphene composites using a novel rapid tooling technique. Rapid Prototyping Journal, 26(4), 765–776. https://doi.org/10.1108/rpj-10-2019-0258
13. Tagimalek, H., & Mahmoodi, M. (2023). *Evaluation of wear test on functionally graded metal-polymer tri-laminate composite interfaces of cooling-assisted friction stir additive manufacturing*. Journal of Advanced Joining Processes, 8, 100166. https://doi.org/10.1016/j.jajp.2023.100166
14. Takayama, S., Saito, Y., Sato, M., Takuya Nagasaka, Takeo Muroga, Ninomiya, Y. (2006). *Sintering Behavior of Metal Powders Involving Microwave-Enhanced Chemical Reaction*. Japanese Journal of Applied Physics, 45(3R), 1816–1816. https://doi.org/10.1143/jjap.45.1816
15. Torralba, J. M., Campos, M. (2014). *Toward high performance in Powder Metallurgy*. Revista de Metalurgia, 50(2), e017. https://doi.org/10.3989/revmetalm.017
16. Touolak, B. T., Nya, F. T. (2014). *More Value of Maroua Clay in the Formulation of Ceramic Products (Terracotta, Earthenware, Stoneware, Porcelain)*. Advances in Materials Physics and Chemistry, 04(12), 284–299. https://doi.org/10.4236/ampc.2014.412031
17. Vakifahmetoglu, C., Karacasulu, L. (2020). *Cold sintering of ceramics and glasses: A review*. Current Opinion in Solid State and Materials Science, 24(1), 100807. https://doi.org/10.1016/j.cossms.2020.100807
18. Vedrtnam, A., Kumar, A. (2017). *Fabrication and wear characterization of silicon carbide and copper reinforced aluminium matrix composite*. Materials Discovery, 9, 16–22. doi.org/10.1016/j.md.2018.01.002
19. Vignesh Babu R., S. Kanagaraj. (2019). *Sintering behaviour of copper/carbon nanotube composites and their characterization*. Advanced Powder Technology, 30(10), 2200–2210. doi.org/10.1016/j.apt.2019.06.035
20. Wang, G., Ruan, Y., Wang, H., Zhao, G., Cao, X., Li, X., Ding, Q. (2023). *Tribological performance study and prediction of copper coated by MoS2 based on GBRT method*. Tribology International, 179, 108149. https://doi.org/10.1016/j.triboint.2022.108149
21. Xu et al. (2016). *Fabrication of tungsten–copper alloys by microwave hot pressing sintering*. Journal of Alloys and Compounds, 658, 23–28. https://doi.org/10.1016/j.jallcom.2015.10.186
22. Zengin, H., Turen, Y., Elen, L. (2019). *A Comparative Study on Microstructure, Mechanical and Tribological Properties of A4, AE41, AS41 and AJ41 Magnesium Alloys*. Journal of Materials Engineering and Performance, 28(8), 4647–4657. https://doi.org/10.1007/s11665-019-04223-8

Received: February 15th, 2024 / Accepted: December 15th, 2024 / Paper available online: December 20th, 2024